



**Acoustics'08
Paris**
June 29-July 4, 2008

www.acoustics08-paris.org

Pure-shear mode BAW resonators consisting of (11-20)textured ZnO films

Takahiko Yanagitani^a, Masato Kiuch^b, Mami Matsukawa^c and Yoshiaki Watanabe^d

^aDepartment of Applied Physics, Nagoya Institute of Technology, 466-8555 Nagoya, Japan

^bNational Institute of Advanced Industrial Science and Technology, 1-8-31 Midorigaoka, Osaka, 563-8577 Ikeda, Japan

^cDoshisha University, 1-3, Tatara Miyakodani, 610-0321 Kyotanabe, Japan

^dFaculty of Engineering, Doshisha Univ., 1-3 Miyakodani Tatara, 610-0321 Kyotanabe, Japan
yanagi@ecei.tohoku.ac.jp

This paper presents pure-shear mode film bulk acoustic wave resonators (FBARs) based on the $(11\bar{2}0)$ textured ZnO and AlN films. We have also introduced FBAR structure consisting of two layers of the $(11\bar{2}0)$ textured ZnO film with opposite polarization directions. This FBAR structure operated in second overtone pure-shear mode, and allowed shear-mode FBARs at higher frequency. For ZnO films, the effective electromechanical coupling coefficients k_{eff}^2 of pure-shear mode FBAR and second overtone pure-shear mode FBAR in this study were found to be 3.3% and 0.8%, respectively. The temperature coefficient of frequency (TCF) for three types of FBARs were measured in the temperature range of 10–60 °C. TCF values of –63.1 ppm/°C, –34.7 ppm/°C, and –35.6 ppm/°C were found for the thickness extensional mode FBAR, the pure-shear mode FBAR, and the second overtone pure-shear mode FBAR, respectively. These results demonstrated that pure-shear mode FBARs have more stable temperature characteristics than the conventional thickness extensional mode FBARs. For AlN films, we report the first synthesis of the $(11\bar{2}0)$ textured AlN film on a silica glass substrate. Shear wave excitation in the GHz range was demonstrated using AlN high overtone bulk acoustic resonator (HBAR) structure.

1 Introduction

Film bulk acoustic resonators (FBARs) have attracted interest not only as telecommunication components but also as sensors in the UHF range [1-5]. (0001) textured ZnO or AlN piezoelectric polycrystalline films have been widely used for the FBARs because their c-axis tends to grow perpendicular to the substrate plane. These (0001) textured FBARs operate in thickness extensional (TE) mode. To excite thickness shear (TS) mode, c-axis tilted ZnO or AlN films have been commonly used. These films operate in quasi-TS mode, and in general, excites quasi-TE mode simultaneously [6-9]. In contrast, $(11\bar{2}0)$ textured films, the crystallites c-axis of which is aligned unidirectionally in the substrate plane, enable excitation of pure-TS mode [10, 11]. Pure-TS mode FBARs have a number of potential advantages compared to TE mode FBARs, such as their more stable temperature characteristics, smaller size, and sensors for liquid-phase.

In this study, TE mode FBAR and pure-TS mode FBAR were fabricated using (0001) textured ZnO films and $(11\bar{2}0)$ textured ZnO films, respectively. We also introduced second-order TS FBAR consisting of two layers of $(11\bar{2}0)$ textured ZnO film with opposite directions of polarization. The second-order mode resonance enables the resonator to operate in a higher frequency range. The temperature characteristics of pure-TS mode FBAR and second-order TS mode FBAR are discussed in comparison with TE mode FBAR.

In addition, this paper reports the first synthesis of the in-plane oriented $(10\bar{1}0)$ and $(11\bar{2}0)$ textured AlN films on a silica glass substrate. Piezoelectric properties of the film were also investigated using high overtone bulk acoustic resonator (HBAR) structure.

2 ZnO film resonator fabrication

Three types of ZnO FBAR samples, labeled samples A, B and C with almost the same film thicknesses were prepared. These samples consisted of Ni electrode layer (0.10 or 0.16 μm)/ZnO piezoelectric layer (5.0 or 5.2 μm)/Al or Cu electrode layer (0.10 or 0.16 μm)/silica glass substrate

(25×75×0.5mm³). Sample A consisted of a (0001) textured ZnO layer, sample B consisted of a $(11\bar{2}0)$ textured ZnO layer, and sample C consisted of two layers of $(11\bar{2}0)$ textured ZnO with opposite polarization. We attempted to fabricate TE mode, pure-TS mode, and second-order pure-TS mode FBARs using samples A, B, and C, respectively.

These ZnO layers were deposited using an RF magnetron sputtering apparatus (RFS-200, Ulvac). The substrate was set outside of the discharge region in (0001) textured layer deposition (off-axis sputtering, sample A), whereas the substrate was set inside the discharge region in $(11\bar{2}0)$ textured layer depositions (on-axis sputtering, samples B and C). During the depositions of the $(11\bar{2}0)$ textured layer, the substrate was moved forward and backward at a speed of 3.2 mm/min. using a vacuum motorized stage, and the substrate was set behind a glass collimator (10×25 mm). This yielded the layers of uniform thickness. The sputtering deposition conditions for the (0001) textured layer and the $(11\bar{2}0)$ textured layer are listed in Table 1. To increase energetic particle bombardment on the film, the $(11\bar{2}0)$ textured layer was deposited under the relatively low sputtering gas pressure of 0.15 Pa. Optimization of deposition conditions for the $(11\bar{2}0)$ textured layer was described previously [12]. In sample C, the layer was deposited twice, as shown in Fig. 1, to obtain two layers with opposite polarizations. The lower ZnO piezoelectric layer was deposited first, and the upper ZnO layer was next deposited after turning the substrate position 180° from the first deposition. Finally, the membrane structures were easily formed by peeling the film layers off the glass substrate.

Table 1 Deposition conditions of the samples.

	Sample A	Sample B	Sample C
Preferred orientation	(0001)	$(11\bar{2}0)$	$(11\bar{2}0)$
Substrate position	Off-axis	On-axis	On-axis
RF power	200 W	200 W	200 W
Substrate temperature	250°C	250°C	250°C
Total gas pressure	0.9 Pa	0.15 Pa	0.15 Pa
Gas composition ratio (Ar/O ₂)	3	1/3	1/3
Deposition rate	1.16 $\mu\text{m}/\text{h}$	1.3 $\mu\text{m}/\text{h}$	1.3 $\mu\text{m}/\text{h}$
Deposition time	4.5 hours	4 hours	2 hours × 2

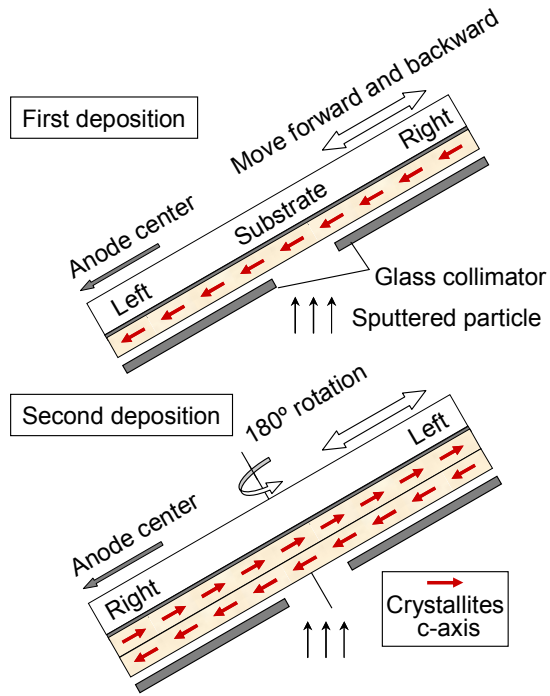


Fig.1 Deposition process of sample C. The layer was deposited twice to obtain two layers with opposite polarization.

3 Characteristics of the ZnO resonators

3.1 Crystallite orientation

In the XRD patterns, an intense (0002) peak was observed in sample A, whereas, (10 $\bar{1}$ 0) and (11 $\bar{2}$ 0) peaks were observed in sample B and C. These results clearly indicated that the crystallite c-axis in the sample A grew perpendicular to the substrate plane, while those in sample B and C grew parallel to the substrate plane. Sample A was expected to excite TE mode, while samples B and C excite pure-TS mode.

The crystallite c-axis orientation in the in-plane direction for sample B and C were determined by X-ray pole figure analysis. The results indicate that the crystallites c-axes in sample B and C are aligned unidirectionally in the anode center-edge direction.

3.2 Frequency response

The input admittance characteristics of samples A, B, and C were measured using a network analyzer (E5071B, Agilent Technologies) through a microwave probe (Picoprobe model 10 GGB Industries). In addition, input admittance characteristics of TE mode FBAR and pure-TS mode FBAR were simulated by one-dimensional Mason's equivalent circuit models [13] including thin electrode layers. Input admittance characteristics of second-order pure-TS mode FBAR consisting of two piezoelectric layers with opposite polarization directions were simulated using modified one-dimensional Mason's equivalent circuit

models as described previously by Saitoh et al. [14]. The density, velocity, and thickness of each layer used for the simulation are listed in Table 2. Longitudinal wave velocity V_l , shear wave velocity V_s , and density ρ of ZnO piezoelectric layers were assumed as ZnO single crystal values [15].

The experimental input admittance characteristics of samples A, B, and C are shown as red solid lines in Figs. 2 (a), (b), and (c), respectively. Intense resonant responses were observed around 554 MHz and 253 MHz for samples A and B, respectively. Comparison of the simulated admittance characteristics (green dashed line) indicates clearly that sample A operates in TE mode and sample B operates in pure-TS mode. In sample A, there is discrepancy between the experimental curve and simulated curve. This may be caused by the error of thickness measurement of the ZnO layer or the difference in longitudinal wave velocity between polycrystalline ZnO and single crystalline ZnO. The effective electromechanical coupling coefficient k_{eff}^2 of TE mode resonator and pure-TS mode resonator, composed of ZnO single crystal, were 8.4% and 6.7%, respectively [15]. The experimental k_{eff}^2 values of TE mode resonance in sample A and of pure-TS mode resonance in sample B were then determined as $k_{l,eff}^2 = 5.9\%$ and $k_{s,eff}^2 = 3.3\%$, respectively. Experimental k_{eff}^2 values of the present resonators were calculated from parallel and series resonant frequencies which are the maximum of the real parts of input impedance and admittance, respectively. In sample B, slight responses appeared at 504 MHz, 546 MHz, and 748 MHz, which correspond to second-order pure-TS mode, fundamental TE mode, and third-order pure-TS mode, respectively. In sample C, intense second-order pure-TS mode was successfully excited. In contrast, the fundamental and third-order pure-TS modes were disappeared entirely. The theoretical k_{eff}^2 value of second-order pure-TS mode was estimated as 5.4%, and a k_{eff}^2 value of 0.8% was obtained experimentally in sample C. As we have seen, although the effective electromechanical coupling coefficient decreases, the second-order harmonic mode operation is one of the ways of increasing operating frequency of FBARs.

Table 2 Properties of each layer in the equivalent circuit model.

	Sample A	Sample B	Sample C
Piezoelectric film	(0001) ZnO	(1120) ZnO	(1120) ZnO
Resonant mode	Thickness extension	Thickness shear	Thickness shear
ρ (kg/m ³)	5665	5665	5665
V (m/s)	6370	2830	2830
l (μ m)	5.2	5.2	2.5+2.5
Top electrode	Ni	Ni	Ni
ρ_{e1} (kg/m ³)	8600	8600	8600
V_{e1} (m/s)	6040	3000	3000
l_{e1} (μ m)	0.16	0.16	0.10
Counterelectrode	Al	Al	Cu
ρ_{e2} (kg/m ³)	2700	2700	8300
V_{e2} (m/s)	6420	3040	2270
l_{e2} (μ m)	0.16	0.16	0.10

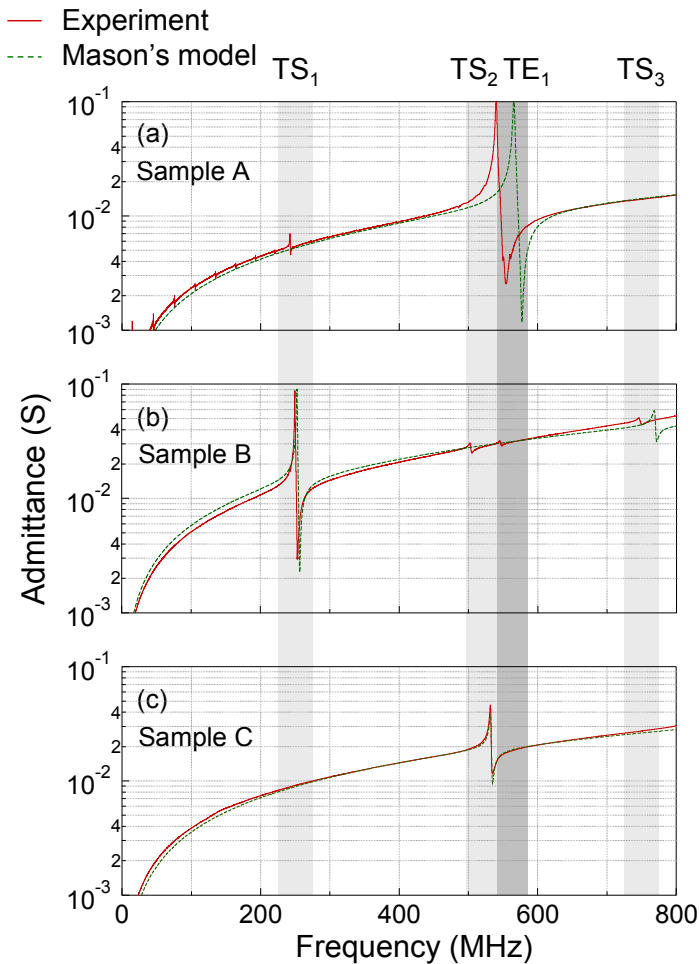


Fig.2 Input admittance characteristics of (a) sample A, (b) sample B, and (c) sample C. These resonator samples have almost same thickness.

3.3 Temperature characteristics

The resonant frequencies of piezoelectric resonators change with temperature due to changes in elasticity and thermal expansion of the piezoelectric layer. The temperature coefficient of frequency (TCF) depends dominantly on the temperature coefficient of the elastic constant, because the thermal expansion effect is one order less than the effect of the change in elasticity. Pure-TS mode ZnO FBAR is expected to exhibit lower TCF than TE mode and quasi-TS mode ZnO FBARs because the temperature coefficient of the elastic constant c_{44} has a smaller value ($-0.69 \times 10^{-4}/^\circ\text{C}$) than c_{33} ($-1.23 \times 10^{-4}/^\circ\text{C}$) for ZnO bulk single crystal (the effects of thermal expansion are included) [16]. The TCF can then be roughly estimated as $-34.5 \text{ ppm}/^\circ\text{C}$ for pure-TS mode resonator and $-61.5 \text{ ppm}/^\circ\text{C}$ for TE mode resonator.

TCF of TE mode FBAR (sample A), fundamental pure-TS mode FBAR (sample B), and second-order pure-TS mode FBAR (sample C) were measured in the temperature range of 10–60 °C using a heating unit (LK-600PM, Japan High Tech). As shown in Fig. 3 (a), (b), and (c), the parallel resonant frequencies of resonators decreased linearly with increasing temperature. By fitting these plots with the linear function, TCF = $-63.1 \text{ ppm}/^\circ\text{C}$ for the TE mode resonator, $-34.7 \text{ ppm}/^\circ\text{C}$ for the fundamental pure-TS mode resonator, and TCF = $-35.6 \text{ ppm}/^\circ\text{C}$ for the second-order pure-TS resonator were determined.

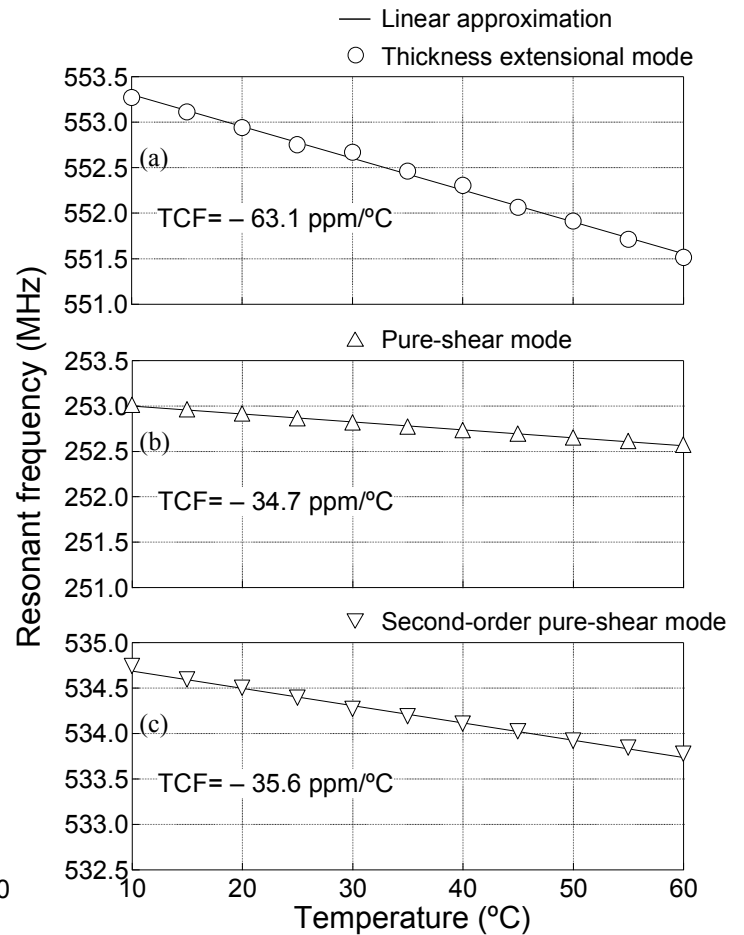


Fig.3 Temperature characteristics of parallel resonant frequency of TE mode FBAR (sample A), pure-TS mode FBAR (sample B), and second-order pure-TS mode FBAR (sample C).

4 $(10\bar{1}0)$ and $(11\bar{2}0)$ AlN film resonators

4.1 $(10\bar{1}0)$ and $(11\bar{2}0)$ textured AlN film

k_s^2 value of the $(11\bar{2}0)$ textured AlN films ($k_s^2 = 2.7\%$) is smaller than that of ZnO films ($k_s^2 = 6.7\%$). However, the acoustic velocity, electrical breakdown strength, and chemical stability in AlN film are better than those in the ZnO films. In addition, temperature coefficient of elastic constant c_{44} and intrinsic acoustic attenuation of the AlN is expected to have smaller value than that of ZnO. These characteristics of AlN film seems to be suitable for FBAR sensors. Synthesis of $(10\bar{1}0)$ textured films have been reported using planar sputtering [17] or ion beam sputter-deposition [18]. We here report the first synthesis of in-plane and out-of plane oriented $(10\bar{1}0)$ or $(11\bar{2}0)$ textured AlN films.

4.2 AlN film deposition

Ion beam sputtering deposition system with single ion gun was used for AlN film deposition. This ion gun plays two roles, sputtering nitrided Al metal target and bombarding

the substrate surface. Nitrogen ion beam with 3 keV was irradiated normal to the target surface and parallel to the substrate surface simultaneously during the deposition. A similar deposition system has been reported for a diamond film deposition [19]. A total gas pressure of 0.02 Pa, and a nitrogen gas flow of 10 ccm were set during deposition. AlN films were deposited on the two types of substrates: silica glass substrate (sample D) and Al electrode film/silica glass structured substrate (sample E). Substrate temperatures during the deposition of sample D and E were around 200 °C and 400 °C, respectively.

4.3 Crystallite orientation

Figure 4 show the XRD patterns of the sample D and E. $(10\bar{1}0)$ and $(11\bar{2}0)$ peaks were observed in the XRD pattern. (0002) peak was not observed in the both sample. FWHM values of the $(11\bar{2}0)$ ω -scan rocking curve were found to be 4.6°. Figure 5 shows the $(11\bar{2}2)$ pole figure of the sample D. FWHM values of ϕ -scan profile curve in $(11\bar{2}2)$ pole of the film were found to be 23°. These results show high in-plane and out-of-plane $(11\bar{2}0)$ preferred orientation.

— AIN/Silica glass - - - JCPDS card No.25-1133 (AIN)
 — AIN/Al/Silica glass - - - JCPDS card No.4-0787 (Al)

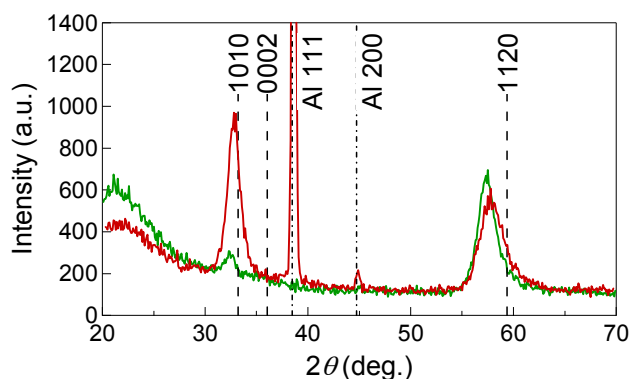


Fig.4 XRD patterns of sample D (AIN/Silica glass) and E (AIN/Al/Silica glass).

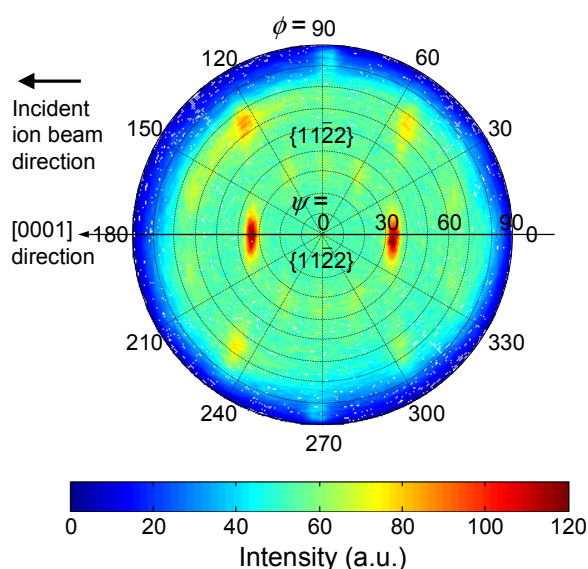


Fig. 5 $(11\bar{2}2)$ pole figure of $(11\bar{2}0)$ textured AIN film (sample D).

4.4 Piezoelectric properties

A Cu film was then evaporated on the sample E as a top electrode of the HBAR. Figure 6 shows the impulse response of the resonator, which was obtained by taking the inverse Fourier transform of the reflection coefficient S_{11} . Shear wave echo train reflected from the bottom substrate surface and the top film surface was clearly observed without any excitation of longitudinal waves.

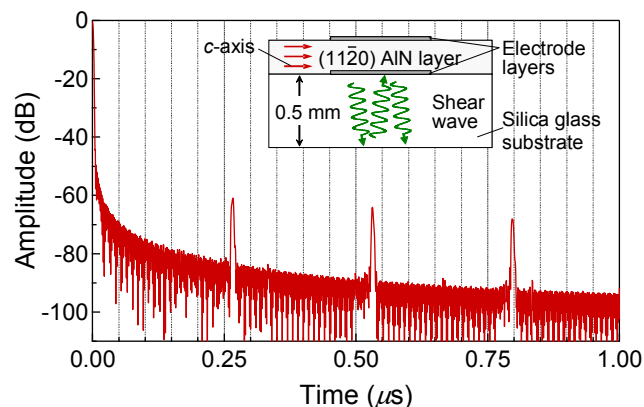


Fig.6 Schematic diagram of pure-TS mode HBAR and impulse response of the resonator. Longitudinal and shear waves propagate in the 0.5-mm-thick silica glass substrate at respective velocities of 3770 m/s and 5960 m/s so that their echoes should be observed at 168 ns and 0.265 ns, respectively.

5 Conclusion

Pure-TS mode FBARs and HBARs consisting of $(11\bar{2}0)$ textured ZnO or AIN films were prepared. The effective electromechanical coupling coefficient k_{eff}^2 of the pure-TS mode ZnO FBAR was estimated as 6.7%. The pure-TS mode ZnO FBAR had a more stable TCF value of -34.7 ppm/°C as compared with the value of -63.1 ppm/°C for the conventional TE mode ZnO FBAR. These results are in good agreement with the estimated ZnO single crystal resonator TCF, -61.5 ppm/°C and -34.5 ppm/°C for TE mode and pure-TS mode, respectively. Furthermore, second-order pure-TS mode FBAR consisting of two layers of $(11\bar{2}0)$ textured ZnO films with opposite directions of polarization were also realized. This resonator showed intensive second-order pure-TS mode resonance without any fundamental or third-order pure-TS modes resonances.

We also demonstrated the shear wave excitation in the GHz range in the $(11\bar{2}0)$ textured AIN HBAR. These AIN films are good candidate for pure-shear mode FBAR and SH-SAW sensors.

References

- [1] R. Ruby, P. Bradley, J. D. Larson III and Y. Oshmyansky, "PCS 1900MHz duplexer using thin film bulk acoustic resonators (FBAR)," *Electron. Lett.*, pp. 794-795, (1999).
- [2] H. P. Loebel, C. Metzmacher, D. N. Peligrad, R. Mauczok, M. Klee, W. Brand, R. F. Milsom, P. Lok, F. van Straten, A. Tuinhout, and J. W. Lobeek, "Solidly mounted bulk acoustic wave filters for the GHz frequency range," in *Proc. IEEE Ultrason. Symp.*, 2002, pp. 897-901.
- [3] T. Nishihara, T. Yokoyama, T. Miyashita, and Y. Satoh, "High performance and miniature thin film bulk acoustic wave filters for 5 GHz," in *Proc. IEEE Ultrason. Symp.*, 2002, pp. 969-972.
- [4] K. M. Lakin, "Thin film resonator technology," *IEEE Trans. Ultrason., Ferroelect., Freq. Contr.*, 52, no. 5, pp. 707-716, (2005).
- [5] M. Benetti, D. Cannata, F. Di Pietrantonio, V. Foglietti and E. Verona, "Microbalance chemical sensor based on thin-film bulk acoustic wave resonators," *Appl. Phys. Lett.*, 87 pp. 173504, (2005).
- [6] J. S. Wang, K. M. Lakin, "c-axis inclined ZnO piezoelectric shear wave films," *Appl. Phys. Lett.*, 42, pp. 352-354, (1983).
- [7] M. Link, M. Schreiter, J. Weber, R. Primig, D. Pitzer, and R. Gabl, "Solidly mounted ZnO shear mode film bulk acoustic resonators for sensing applications in liquids," *IEEE Trans. Ultrason., Ferroelect., Freq. Contr.*, 53, pp. 492-496, (2006).
- [8] F. Martin, M.-E. Jan, S. Rey-Mermet, B. Belgacem, D. Su, M. Cantoni, and P. Muralt "Shear mode coupling and tilted grain growth of AlN thin films in BAW resonators," *IEEE Trans. Ultrason., Ferroelect., Freq. Contr.*, 53, pp. 1339-1343, (2006).
- [9] J. Bjurström, G. Wingqvist, and I. Katardjiev, "Synthesis of textured thin piezoelectric AlN films with a nonzero c-axis mean tilt for the fabrication of shear mode resonators" *IEEE Trans. Ultrason., Ferroelect., Freq. Contr.*, 53, pp. 2095-2100, (2006).
- [10] T. Yanagitani, T. Nohara, M. Matsukawa, Y. Watanabe and T. Otani, "Characteristics of (10 $\bar{1}$ 0) and (11 $\bar{2}$ 0) textured ZnO piezofilms for a shear mode resonator in the VHF-UHF frequency ranges," *IEEE Trans. Ultrason., Ferroelect., Freq. Contr.*, 52, pp. 2140-2145, (2005).
- [11] T. Yanagitani, M. Kiuchi, M. Matsukawa, and Y. Watanabe, "Shear mode electromechanical coupling coefficient k_{15} and crystallites alignment of (11 $\bar{2}$ 0) textured ZnO films," *J. Appl. Phys.* 102, 024110, (2007).
- [12] T. Kawamoto, M. Matsukawa, Y. Watanabe and T. Yanagitani, "Study on formation mechanism of (11 $\bar{2}$ 0) textured ZnO films," in *Proc. IEEE Ultrason. Symp.*, 2006, pp. 1529-1532.
- [13] W. P. Mason, in *Physical Acoustics*, vol. 1 Part A, (Academic New York 1964).
- [14] S. Saitoh, M. Izumi, and Y. Mine, "A Dual Frequency Ultrasonic Probe for Medical Applications," *IEEE Trans. Ultrason., Ferroelect., Freq. Contr.*, 42, pp. 294-300, (1995).
- [15] R. T. Smith and V. E. Stubblefield, "Temperature dependence of the electroacoustical constants of Li-doped ZnO single crystals," *J. Acoust. Soc. Am.*, 46, p. 105, (1969).
- [16] E. F. Tokarev, I. B. Kobayakov, I. P. Kuz'mina, A. N. Lobachev and G. S. Pado, "Elastic, dielectric, and piezoelectric properties of zincite in the 4.2-800°K temperature range," *Sov. Phy. Solid State*, 17, pp. 629-632, (1975).
- [17] F. Takeda, T. Mori, and T. Takahashi, "Effect of hydrogen gas on c-axis oriented AlN films prepared by reactive magnetron sputtering," *Jpn. J. Appl. Phys.*, 20, L169-171, (1981).
- [18] J. M. E. Harper, J. J. Cuomo, and H. T. G. Hentzell, "Quantitative ion beam process for the deposition of compound thin films," *Appl. Phys. Lett.*, 43 pp. 547-549, (1983).
- [19] M. Kitabatake and K. Wasa, "Diamond films by ion-assisted deposition at room temperature," *J. Vac. Sci. Technol. A* 6, 1793-1797, (1988).